Cell Host & Microbe
Article

Functional Dissection of the Apicomplexan Glideosome Molecular Architecture

Karine Frénal,[1] Valérie Polonais,[1] Jean-Baptiste Marq,[1] Rolf Stratmann,[2] Julien Limenitakis,[1] and Dominique Soldati-Favre[1,*]
[1]Department of Microbiology and Molecular Medicine, Centre Medical Universitaire, University of Geneva, 1 Rue Michel-Servet, CH-1211 Geneva 4, Switzerland
[2]Nationale Kontaktstelle Lebenswissenschaften, Projektträger Jülich und Projektträger im Deutschen Zentrum für Luft- und Raumfahrt, Heinrich-Konen-Strasse 1, 53227 Bonn, Germany
*Correspondence: dominique.soldati-favre@unige.ch
DOI 10.1016/j.chom.2010.09.002

SUMMARY

The glideosome of apicomplexan parasites is an actin- and myosin-based machine located at the pellicle, between the plasma membrane (PM) and inner membrane complex (IMC), that powers parasite motility, migration, and host cell invasion and egress. It is composed of myosin A, its light chain MLC1, and two gliding-associated proteins, GAP50 and GAP45. We identify GAP40, a polytopic protein of the IMC, as an additional glideosome component and show that GAP45 is anchored to the PM and IMC via its N- and C-terminal extremities, respectively. While the C-terminal region of GAP45 recruits MLC1-MyoA to the IMC, the N-terminal acylation and coiled-coil domain preserve pellicle integrity during invasion. *GAP45* is essential for gliding, invasion, and egress. The orthologous *Plasmodium falciparum GAP45* can fulfill this dual function, as shown by transgenera complementation, whereas the coccidian GAP45 homolog (designated here as) *GAP70* specifically recruits the glideosome to the apical cap of the parasite.

INTRODUCTION

Toxoplasma gondii is an obligate intracellular parasite that belongs to the group of *Apicomplexa*, causing severe disease in humans and animals. Together with the other chromalveolates, they possess an unusual pellicle composed of flattened cisternae forming the inner membrane complex (IMC), which closely apposes to the plasma membrane (PM). On its other side, the IMC is intimately associated with a network of intermediate filament-like proteins and subpellicular microtubules (Morrissette et al., 1997). The IMC displays a highly ordered distribution of inner membrane particles (IMPs) as observed by illuminating freeze fracture studies (Dubremetz and Torpier, 1978). The IMC is either continuous or composed of patches of flattened vesicles joined together by sutures. Additionally, in coccidians, the apical cap (defined as the most apical plate of the IMC) precisely delineates a subdomain of the IMC displaying a distinct internal structure (Dubremetz and Torpier, 1978). On live *Eimeria* sporozoites, the apical cap was shown to be more flexible than the remainder of the body and hence to be able to undergo successive elongation and retraction (Dubremetz and Torpier, 1978).

In apicomplexans, most invasive stages rely on an unusual form of substrate-dependent motility that assists them in crossing nonpermissive biological barriers and in actively penetrating and exiting host cells. Gliding motility is powered by an actomyosin-motor and requires the coordinate action of a multiprotein machine termed the "glideosome" (Opitz and Soldati, 2002). Assembly of the glideosome is precisely orchestrated in time and space and confined to the narrow region between the PM and IMC (Keeley and Soldati, 2004). Gliding motility requires actin polymerization (Wetzel et al., 2003) and a motor complex composed of the class XIV myosin A (MyoA), its associated myosin light chain 1, MLC1 or MTIP (Bergman et al., 2003; Herm-Götz et al., 2002), and two gliding-associated proteins, GAP45 and GAP50 (Gaskins et al., 2004). GAP45 is modified by myristoylation and palmitoylation, whereas GAP50 is an integral membrane protein of the IMC, and both were proposed to anchor MyoA to the IMC (Gaskins et al., 2004). The precomplex MyoA-MLC1-GAP45 is anchored to the IMC through association with GAP50 and acylation of GAP45 (Gaskins et al., 2004; Rees-Channer et al., 2006). GAP50 is firmly immobilized in the IMC and was proposed to act as a fixed anchor for the motor complex (Johnson et al., 2007).

Here, we first identified a fifth component of the glideosome named GAP40. This polytopic IMC protein is conserved across the phylum of *Apicomplexa*. We also show that the N-terminal domain of MLC1 serves as a tail for MyoA and brings the motor to its site of action by association with the C terminus of GAP45. Unexpectedly, the N-terminal lipid modification of GAP45 anchors the protein to the PM. To understand the significance of this association with the PM, we undertook a functional dissection of GAP45. As anticipated, an inducible knockout of the *TgGAP45* gene revealed a profound impairment in parasite gliding, invasion, and egress. Scrutiny of the phenotype unraveled the crucial role played by GAP45 in the recruitment of the motor complex at the pellicle. Moreover, morphological analysis uncovered a second role for GAP45 in maintaining the cohesion of the pellicle during invasion. Mutants affected in N-terminal acylation underscore the contribution of GAP45 in pellicle integrity. These facets of GAP45 function are conserved in

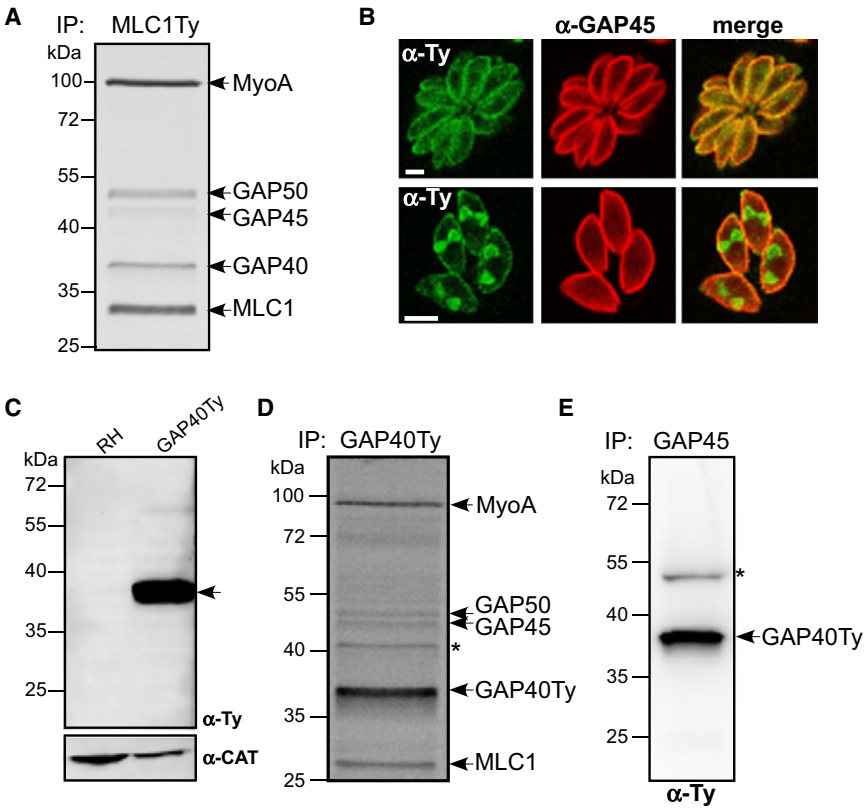

Figure 1. Identification of a Gliding-Associated Protein, GAP40

(A) [^{35}S]-labeled methionine/cysteine parasites stably expressing MLC1Ty were subjected to IP with anti-Ty antibody. Eluted proteins were visualized by autoradiography. A protein below 40 kDa was precipitated in addition to the other known glideosome components and was named GAP40 (GenBank HM751080).

(B) The localization of GAP40Ty was determined in intracellular parasites with anti-Ty (green) and anti-GAP45 (red). Scale bars represent 2 μm.

(C) Total lysates from RH parasites expressing GAP40Ty or not were analyzed by western blot with anti-Ty. Catalase (CAT) was used as a loading control.

(D) Parasites expressing GAP40Ty were labeled with [^{35}S]-methionine/cysteine and IP with anti-Ty antibodies. Immune complexes were visualized by autoradiography. The asterisk indicates an unknown protein.

(E) Parasites expressing GAP40Ty were subjected to IP with anti-GAP45 antibodies, and the presence of GAP40Ty in the elution was checked by western blot. The asterisk indicates the IgG heavy chains that cross-reacted with the secondary antibodies.

See also Figure S1.

P. falciparum GAP45 and in the homolog GAP70, which specifically recruits the glideosome to the apical cap in coccidians.

RESULTS

GAP40 Is a Polytopic IMC Protein that Belongs to the Glideosome

When ^{35}S-methionine and cysteine metabolically labeled MLC1-Ty-expressing parasites are subjected to coimmunoprecipitation (coIP), five bands that correspond to the components of the glideosome are visible (Figure 1A). This profile was described earlier, and the prominent 40 kDa band was assigned to a breakdown product of GAP45 (Gaskins et al., 2004). However, antibodies raised against the entire GAP45 protein failed to recognize this product, prompting us to perform a mass spectrometry analysis on a preparative purification of the glideosome (Figure S1A available online). The presence of two peptides corresponding to a hypothetical protein with a predicted mass of 43 kDa was investigated further. The generation of transgenic parasites expressing a C-terminal tagged version of this protein identified a resident polytopic protein of the IMC with an apparent molecular weight of ~37 kDa (Figures 1B and 1C). CoIP performed with anti-Ty formally established the association of this protein with the MyoA-MLC1-GAP45-GAP50 complex (Figure 1D), and, conversely, a coIP performed with anti-GAP45 antibodies precipitated the Ty-tagged protein (Figure 1E). Taken together, these results confirm the identification of a member of the glideosome, named GAP40. *GAP40* is highly conserved across the phylum of *Apicomplexa* (Figure S1B), and in *P. falciparum*, expression of PFE0785c peaks in late schizonts.

The N-Terminal Domain of MLC1 Is Implicated in the Assembly of MyoA with the GAPs

The four EF-hand motifs, which compose the calmodulin (CaM)-like domain of MLC1 (CtMLC1), are necessary and sufficient to bind to the degenerated IQ motif at the C terminus of MyoA in a calcium-independent manner (Bosch et al., 2007; Green et al., 2006). The unusual N-terminal extension of MLC1 (NtMLC1) (Herm-Götz et al., 2002) was fused to GFPTy (NtMLC1GFPTy) and was shown to distribute at the parasite periphery like MLC1, whereas CtMLC1GFPTy was essentially cytosolic (Figure 2B and Figure S2). To discriminate between an association with the IMC or the PM, we treated extracellular tachyzoites with the pore-forming *Aeromonas hydrophila* aerolysin as previously described with alpha-toxin (Wichroski et al., 2002). Both MLC1Ty and NtMLC1GFPTy partitioned with the IMC, colocalizing with GAP45, like the endogenous MLC1 (Figure S2B). These data suggested that NtMLC1 is acting as an important determinant for the localization of the motor to the pellicle. To confirm these results, we performed coIPs of MLC1-GFP fusions on the transgenic parasite lines and monitored association with the other components of the glideosome by western blot analysis (Figure 2C). NtMLC1GFPTy interacted with GAP45, whereas CtMLC1GFPTy binds to MyoA, as previously reported (Bergman et al., 2003). The absence of direct

interaction between MyoA and the GAPs was confirmed by metabolic labeling of CtMLC1GFPTy-expressing parasites followed by coIP (Figure 1D). These results do not rule out the possibility that MyoA interacts with the GAPs once it is successfully recruited to the pellicle. Additionally, the data cannot discriminate whether NtMLC1 and/or GAP45 is involved in a direct interaction with the IMC.

GAP45 Mediates the Interaction of MLC1-MyoA with the Pellicle

To determine which residues in this region bind to GAP45, we generated two sets of site-specific mutations in stretches of amino acids conserved in all apicomplexan MLC1/MTIP (Figure 2E and Figure S2C). Both MLC1DE-AATy and MLC1PGE-AIATy mutants were predominantly cytosolic. To determine the impact of these mutations on the assembly of the motor complex, we performed coIPs on parasites metabolically labeled with ^{35}S-methionine and cysteine (Figure 1F). These mutants assembled with MyoA, indicating that the CaM-like domain was appropriately folded but failed to bind to GAP45, suggesting that the conserved residues were either critical for interaction with GAP45 or for proper folding of the N-terminal extension. The two conserved cysteine residues, C8 and C11, are predicted to be palmitoylated by CSS-Palm 2.0 (Ren et al., 2008) with scores of 1.83 and 1.65, respectively. To determine whether acylation could contribute to the anchoring of MLC1 to the IMC, we replaced the two cysteines with alanine residues. The resulting mutant MLC1CC-AATy was cytosolic but simultaneously impaired in binding to GAP45, leaving open the possibility that MLC1 is acylated. Collectively, these results confirmed that the proper targeting of MLC1 correlates with its ability to associate to GAP45 and that these two features could not be separated.

GAP45 Is Dually Anchored to the Two Components of the Pellicle

The N-terminal conserved sequence of GAP45 carries predicted myristoylation and palmitoylation sites, and in *Plasmodium*, PfGAP45 was experimentally shown to be acylated (Rees-Channer et al., 2006). Two more palmitoylation sites are predicted within the C-terminal conserved region of GAP45 (Figures S3A and S3B). In order to identify the key determinant(s) responsible for localization of GAP45 to the pellicle, we mutated the N-terminal acylation sites and introduced a Ty-tag at the C terminus of GAP45, which was previously reported to prevent its assembly with the glideosome (Johnson et al., 2007). Alternatively, we inserted a Myc-tag upstream of the coiled-coil region to avoid interference with the function of the C-terminal region (Figure S3C). GAP45Ty localized to the periphery of the parasites as shown by the colocalization with MLC1, whereas the N-terminal acylation mutant GC-AAGAP45Ty was cytosolic (Figure 3A). Rather unexpectedly, this mutant behaved drastically differently when the tag was replaced by Myc positioned upstream of the coiled-coil domain. GC-AAMycGAP45 assembled together with MLC1 and MyoA and was found to be associated with mature as well as nascent daughter cell IMCs, a localization never observed for the components of the glideosome except GAP50 and GAP40 (Gaskins et al., 2004; Rees-Channer et al., 2006). In the light of these results, we postulate that the N-terminal acylations of GAP45 target the motor complex preferentially to the PM prior to anchoring into the IMC, thereby avoiding association with the nascent IMCs. To test this hypothesis, we investigated whether GAP45Ty was associated with the IMC or PM by treating extracellular tachyzoites with aerolysin prior to immunofluorescence assay (IFA). Consistent with our hypothesis, GAP45Ty was found to be associated mainly with the PM. A fraction of GAP45Ty also appeared to be located in the space between the IMC and the PM under toxin treatment, possibly because the anchorage is reversible, a typical characteristic of palmitoylation (Figure 3B). In comparison, MycGAP45 behaved like endogenous GAP45 and was located on the outer leaflet of the IMC (Gaskins et al., 2004). In this case, the interaction of GAP45 with the IMC is more robust and hence dictates the collapse of the complex to the IMC side of the pellicle. The results obtained by IFAs were confirmed by fractionation experiments. Like GAP45, MycGAP45 and GAP45Ty were completely soluble only in the presence of detergent, whereas GC-AAGAP45Ty was readily soluble in PBS and GC-AAMycGAP45 could be solubilized in Na_2CO_3 pH 11.0 (Figure 3C). Taken together, these data established that GAP45 is anchored to the PM by N-terminal acylation and to the IMC via the intact C terminus. The N-terminal acylation prevents the association of MyoA to the nascent IMCs of the daughter cells, suggesting that acylation is important for insertion of the motor to the pellicle in a temporally controlled manner.

The C Terminus of GAP45 Binds to the Motor and Anchors It to the IMC

Like the extreme N terminus, the C-terminal block of GAP45 is a strikingly conserved part of the protein across the Apicomplexa phylum (Figure S3A). To investigate its contribution to glideosome assembly and targeting to the IMC, we fused this region at the C terminus of a Myc-GFP (Figure S3C). The resulting MycGFPCt-GAP45 protein localized to the IMC of both mature parasites and daughter cells (Figure 4A). Under these conditions, MLC1 was also observed in the nascent IMCs via interaction with the chimeric GFP (Figure 4A), which was confirmed by coIPs (Figure 4B).

The CtGAP45 encompasses a CXXC sequence with a weak score for a predictable type II palmitoylation site (Ren et al., 2008) (Figure S3B). To test whether these two cysteine residues were critical for anchoring GAP45 to the IMC, we introduced the double C230A and C233A mutations into MycGFPCtGAP45. The resulting MycGFPCtGAP45CC-AA protein was cytosolic (Figure 4A), pointing to an involvement of the two cysteines either in lipid modifications or in direct interaction with GAP50 and/or GAP40. When the two mutations were introduced into Myc-GAP45, MycGAP45CC-AA was still found at the pellicle (Figure 4C), but this time, like in the case of GAP45Ty, the protein was associated preferentially with the PM as revealed by aerolysin treatment (Figure 4D). MycGAP45CC-AA was still able to assemble with the motor complex; however, the interaction with MLC1 occurred selectively with the slower migrating form of MLC1 (Figure 4B). It is plausible that the absence of a direct connection between GAP45 and IMC interferes with posttranslational modifications on MLC1. This aspect will require further investigation.

Collectively, the analysis of the mutants depicted in Figure 4E led us to conclude that the CtGAP45 is involved in the assembly

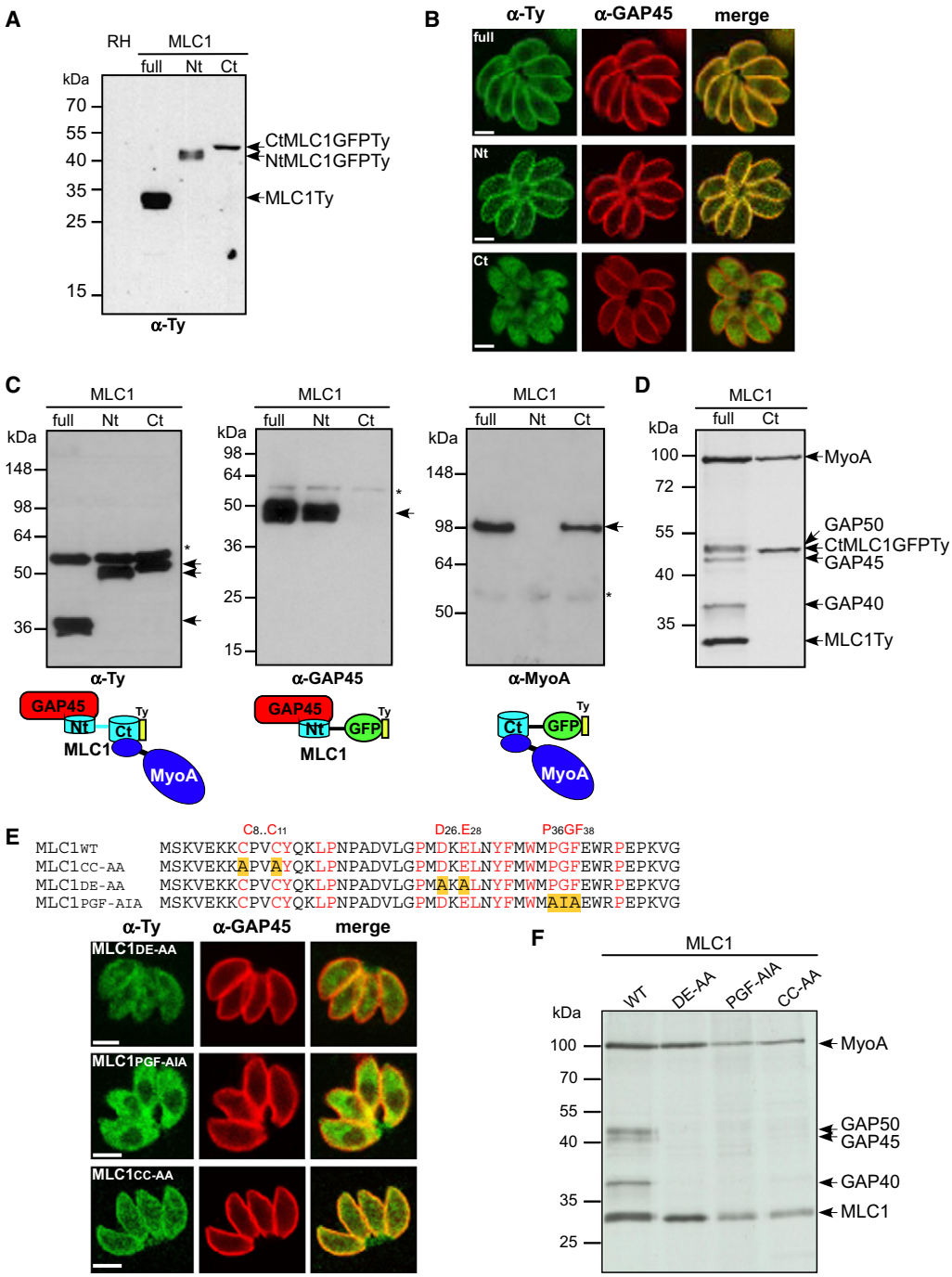

Figure 2. GAP45 Is Associated to the Motor by Interacting with the N-Terminal Extension of MLC1

(A) Total lysates from RH strain parasites stably expressing MLC1Ty (full), NtMLC1GFPTy (Nt), and CtMLC1GFPTy (Ct) were analyzed by western blot with anti-Ty.

(B) The subcellular localization of MLC1 full, Nt, and Ct in intracellular tachyzoites was determined by IFA with anti-Ty antibody. GAP45 stained the periphery of the parasites. Scale bars represent 2 μm.

(C) Extracellular parasites stably expressing MLC1 full, Nt, and Ct were subjected to IPs with anti-Ty antibodies. The immune complexes were analyzed by western blot with anti-Ty (left), anti-GAP45 (middle), and anti-MyoA (right). Asterisks indicate the IgG heavy chains that cross-reacted with the secondary antibodies. Schemes recapitulate the interactions within the glideosome according to the MLC1 construct expressed by the parasites.

(D) Parasites expressing MLC1 full and Ct were labeled with [^{35}S]-methionine/cysteine and IP with the anti-Ty antibody. Elutions were visualized by autoradiography.

(E) Point mutations introduced in MLC1 N terminus are highlighted in yellow, and residues that are identical in apicomplexan MLC1/MTIP N-terminal extension according to the multiple alignments performed in Figure S2C are labeled in red. The localization of MLC1 mutants in intracellular tachyzoites was assessed by IFA with anti-Ty. Anti-GAP45 was used to visualize the periphery of the parasites. Scale bars represent 2 μm.

of the glideosome and that the conserved cysteine residues are crucially implicated in the anchoring of GAP45 to the IMC but not in the recruitment of MLC1-MyoA.

GAP45 Is Essential for Motility, Invasion, and Egress

The unanticipated topology of GAP45 spanning the PM and IMC prompted us to investigate the contribution of GAP45 in glideosome function and in particular to assess the importance of the N-terminal acylations. To this aim, a conditional knockout of *GAP45* was generated with an inducible system (Meissner et al., 2002). At first, an inducible copy of MycGAP45 was introduced in a TATi-1 strain to generate the GAP45e/GAP45i parasite line. Then, deletion of the endogenous locus was performed by double homologous recombination to obtain the ΔGAP45e/GAP45i strain (Figure S4A). Efficient depletion of MycGAP45 in GAP45e/GAP45i and ΔGAP45e/GAP45i was monitored by western blot and by IFA, 48 hr after incubation with anhydrotetracycline (ATc) (Figures 5A and 5B). In the absence of GAP45i, MLC1 was dramatically redistributed to the cytosol, validating the hypothesis that GAP45 is a prerequisite for the recruitment of MLC1-MyoA to the IMC (Figure 5B). The phenotypic consequence of GAP45 depletion was first evaluated by plaque assay, 6 days after inoculation of human foreskin fibroblasts (HFFs). In contrast to TATi-1 and GAP45e/GAP45i, ΔGAP45e/GAP45i showed evidence of a severe defect in one or more steps of the lytic cycle in the presence of ATc (Figure 5C). Intracellular growth was estimated by counting the number of parasites per vacuole, 48 hr after ATc treatment. All strains showed a comparable rate of parasite division, excluding a role for GAP45 in this process (Figure S4B). Moreover, no defect in organelle biogenesis (micronemes, rhoptries, mitochondrion) and no apparent defect in IMC biogenesis and pellicle integrity were observed (Figure S4C). In contrast, an impaired recruitment of MyoA to the pellicle is anticipated to profoundly compromise all the events implicated in glideosome function. When depleted in GAP45i, ΔGAP45e/GAP45i failed to form detectable trails in a gliding assay (Figure S4D). TATi-1, GAP45e/GAP45i, and ΔGAP45e/GAP45i were also treated for 57 hr with ATc and induced to egress by addition of the calcium-ionophore A23187. Depletion of GAP45 caused a dramatic defect in egress with less than 10% of the vacuoles ruptured (Figure 5G). Similarly, invasion efficiency of ΔGAP45e/GAP45i was reduced to 25% relative to the GAP45e/GAP45i or TATi-1 strains (Figure S4E).

Molecular Dissection of GAP45 Function by Complementation

The severe phenotype observed upon GAP45 depletion offered a unique opportunity to functionally assess the specific features of GAP45 including the importance of N-terminal acylations, the length and rigidity of the coiled-coil domain, and the association with the IMC. To this goal, a series of vectors expressing diverse GAP45 mutants were created (Figure S5A) and analyzed (Table S1). The ability of these constructs to functionally complement ΔGAP45e/GAP45i was first evaluated using ATc as a selectable marker, as previously described for the complementation of the profilin knockout (Plattner et al., 2008). Parasites expressing MycGAP45, MycGFPGAP45, and the *P. falciparum* homolog TyPfGAP45 were readily obtained and cloned under ATc selection. GAP45i was shown to be still regulated in these clones, except for MycGAP45, which could not be distinguished from GAP45i (Figure 5D). In all the ATc-complemented strains, the localization of MLC1 to the pellicle was restored, as shown by IFA on parasites treated with ATc for 48 hr (Figure 5E). Consistent with these results, the strains formed normal plaques in the presence of ATc (Figure 5F), and the defect in egress was restored to the wild-type level (Figure 5G). In contrast, parasites expressing GAP45Ty could not be obtained under ATc selection. Since the presence of a Ty-tag interferes with the recruitment of MyoA-MLC1, we conclude that this facet of GAP45 activity is critical for glideosome function.

A Dual Role for GAP45 in Glideosome Function

The constructions that failed to rescue the depletion of GAP45i were introduced into ΔGAP45e/GAP45i via phleomycin selection (Black et al., 1995). The regulation of GAP45i was checked by western blot analysis (Figure 6A) and IFA (Figure S5B). As previously observed in RH, GAP45 mutated in the N-terminal acylation sites (GC-AAMycGAP45) caused a premature assembly of MLC1 to the nascent IMC of the daughter cells. Although the motor complex is assembled at the pellicle (Figure 6B), this mutant failed to complement GAP45i depletion as monitored by plaque assay (Figure 6C). Expression of GC-AAMycGAP45 showed an intermediate phenotype in the egress assay (Figure 6D), and those parasites able to break the host cell membrane did not spread as efficiently as fully rescued mutants. Further investigation of this mutant with an intracellular growth assay performed in the presence of ATc confirmed that the premature association of the motor with nascent IMCs caused no deleterious consequences for replication (Figure S5D). These results establish that the recruitment of the motor to the pellicle is not the sole vital role of GAP45, and the importance of its anchoring in the PM suggests a role in maintaining the cohesion of the pellicle during invasion. To confirm the role of GAP45 in holding the pellicle together during invasion, we designed two mutants affecting the length and rigidity of the coiled-coil domain. Deletion of the coiled-coil domain (TyGAP45Δcoil) or its duplication (TyGAP45-2coils) failed to complement ΔGAP45e/GAP45i, as shown by the inability of the phleomycin selected clones to form plaques in presence of ATc (Figure 6C). TyGAP45Δcoil and MLC1 were correctly inserted into the pellicle both in the presence and absence of ATc (Figure 6B and Figure S5B). In contrast, accessibility of TyGAP45-2coils to the pellicle was significantly reduced in the absence of GAP45i, and the protein tended to accumulate as small dots throughout the parasite (Figure 6B and Figure S5B). Under this circumstance, TyGAP45-2coils failed to recruit quantitatively the motor to the pellicle. Examination of the intracellular growth

(F) [^{35}S]-labeled methionine/cysteine parasites stably expressing MLC1Ty, MLC1DE-AATy, MLC1PGE-AIATy, and MLC1CC-AATy were subjected to IPs with anti-Ty antibodies. Eluted proteins were visualized by autoradiography.
See also Figure S2.

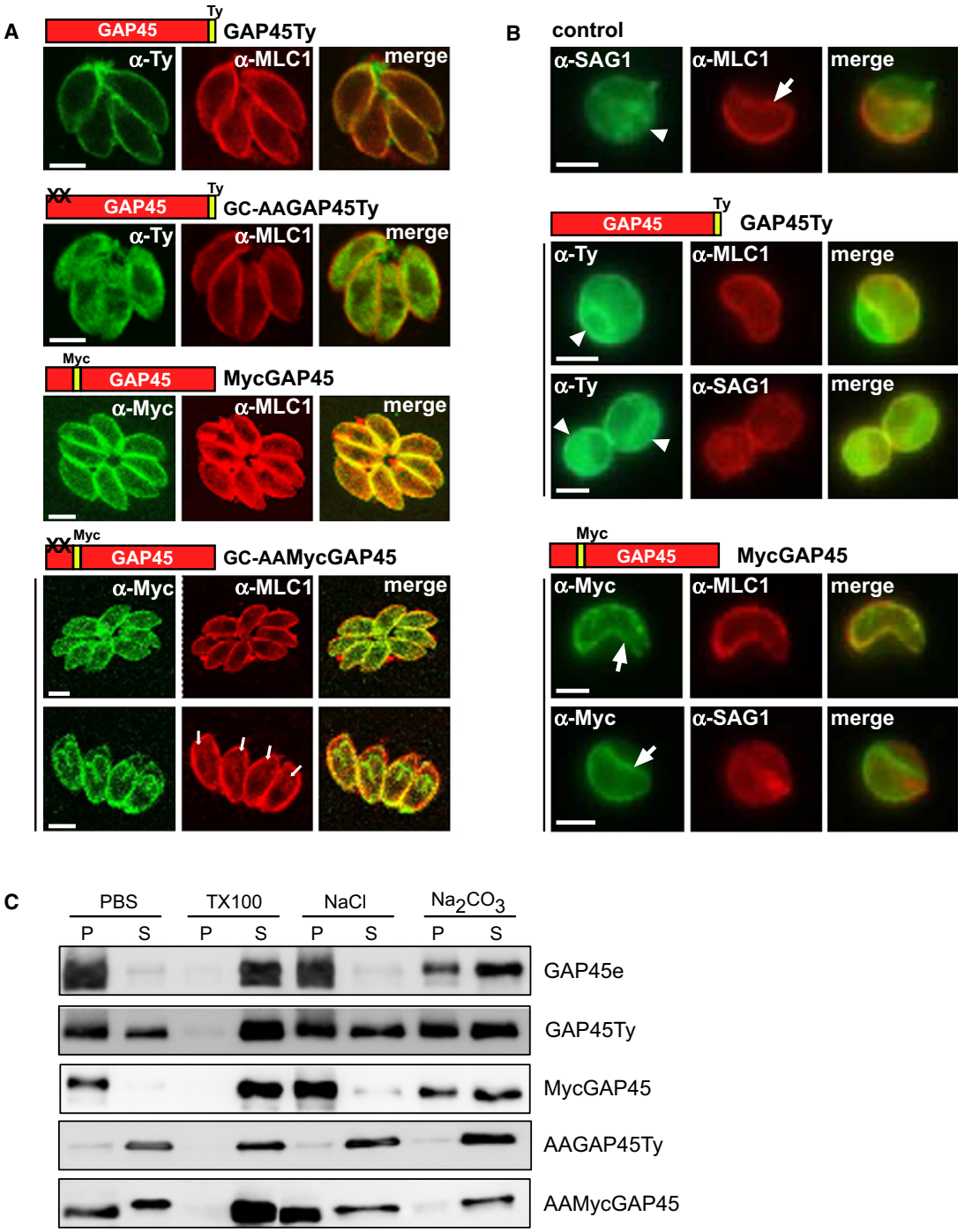

Figure 3. GAP45 Is Dually Anchored to the Pellicle

(A) The localization of GAP45Ty, GC-AAGAP45Ty, MycGAP45, and GC-AAMycGAP45 in intracellular parasites was determined by IFA with anti-Ty or anti-Myc. The periphery of the parasite was visualized by anti-MLC1 staining. White arrows point to MLC1 localization at the IMC of growing daughter cells. Scale bars represent 2 μm.

(B) The distribution of GAP45Ty and MycGAP45 in the pellicle was determined in extracellular tachyzoites treated with *A. hydrophila* aerolysin using anti-Ty and anti-Myc antibodies, respectively. Anti-MLC1 was used to visualize the IMC (arrows), whereas anti-SAG1 stained the PM (arrowheads). Scale bars represent 2 μm.

(C) The solubility of endogenous GAP45 (GAP45e) and recombinant constructs was studied by fractionation after extraction in PBS, PBS/TX100, PBS/NaCl, or PBS/Na_2CO_3. Their distribution in different fractions was assessed by western blot with anti-GAP45, anti-Ty, or anti-Myc antibody.

See also Figure S3.

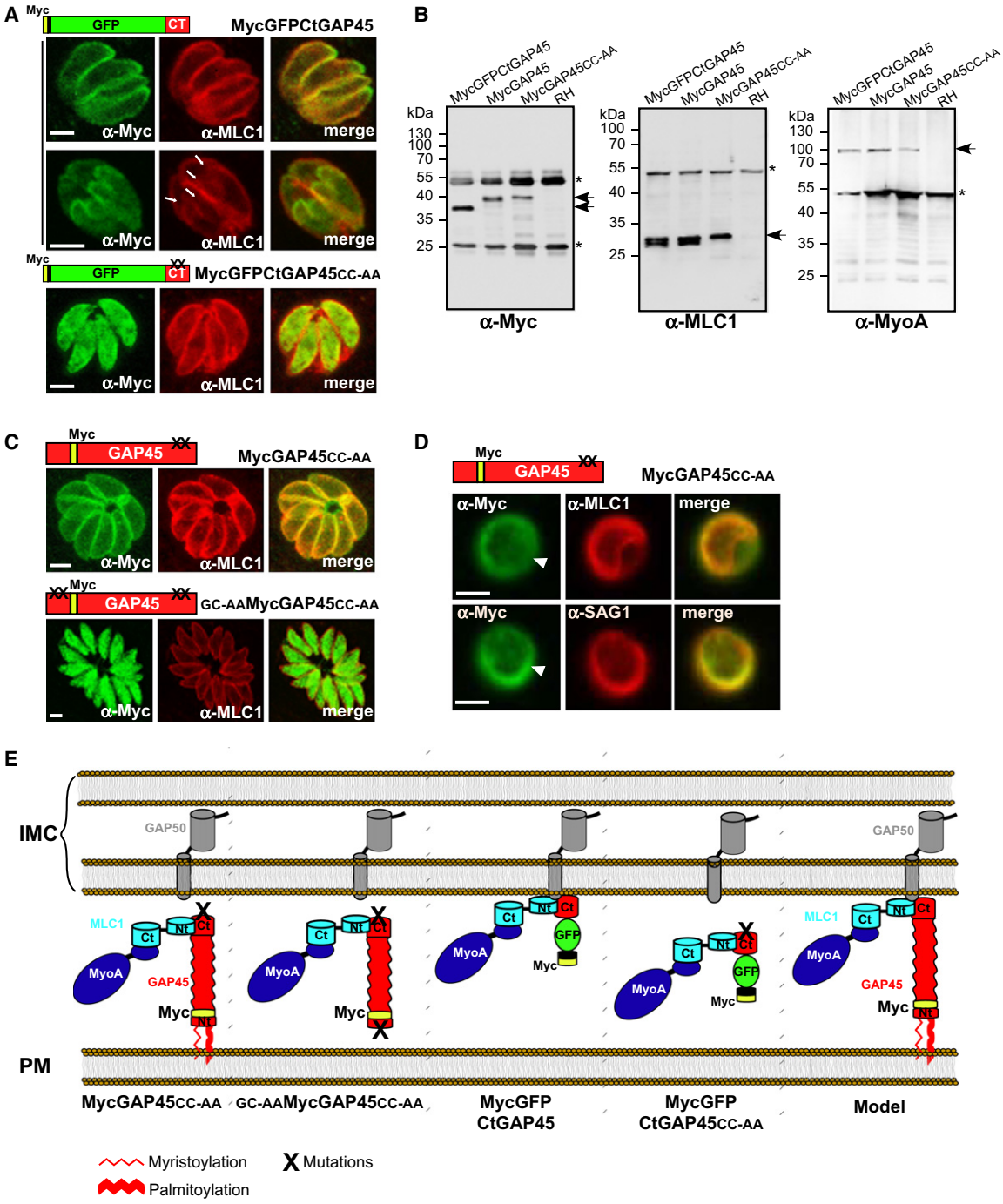

Figure 4. The Conserved C-Terminal Domain of GAP45 Is Essential for Interaction with the IMC and MLC1-MyoA

(A) The localization of MycGFPCtGAP45 and MycGFPCtGAP45CC-AA in intracellular tachyzoites was assessed by IFA with anti-Myc and anti-MLC1 antibodies. White arrows point the localization of MLC1 at the nascent IMC of daughter cells. Scale bars represent 2 μm.

(B) Extracellular parasites stably expressing MycGFPCtGAP45, MycGAP45, MycGAP45CC-AA, and RH were subjected to IPs with anti-Myc antibodies. Elutions were analyzed by western blot for the presence of Myc-tagged proteins (left), MLC1 (middle) and MyoA (right).

(C) The localization of MycGAP45CC-AA and GC-AAMycGAP45CC-AA in intracellular parasites was determined by IFA with anti-Myc and anti-MLC1 antibodies. Scale bars represent 2 μm.

(D) The distribution of MycGAP45CC-AA at the pellicle was determined in extracellular tachyzoites treated with aerolysin using anti-Myc antibody. IMC and PM (arrowhead) were labeled with anti-MLC1 and anti-SAG1, respectively. Scale bars represent 2 μm.

(E) Schematic representation of the glideosome motor complex anchorage at the pellicle according to the GAP45 construct expressed by the parasites.

See also Figure S3.

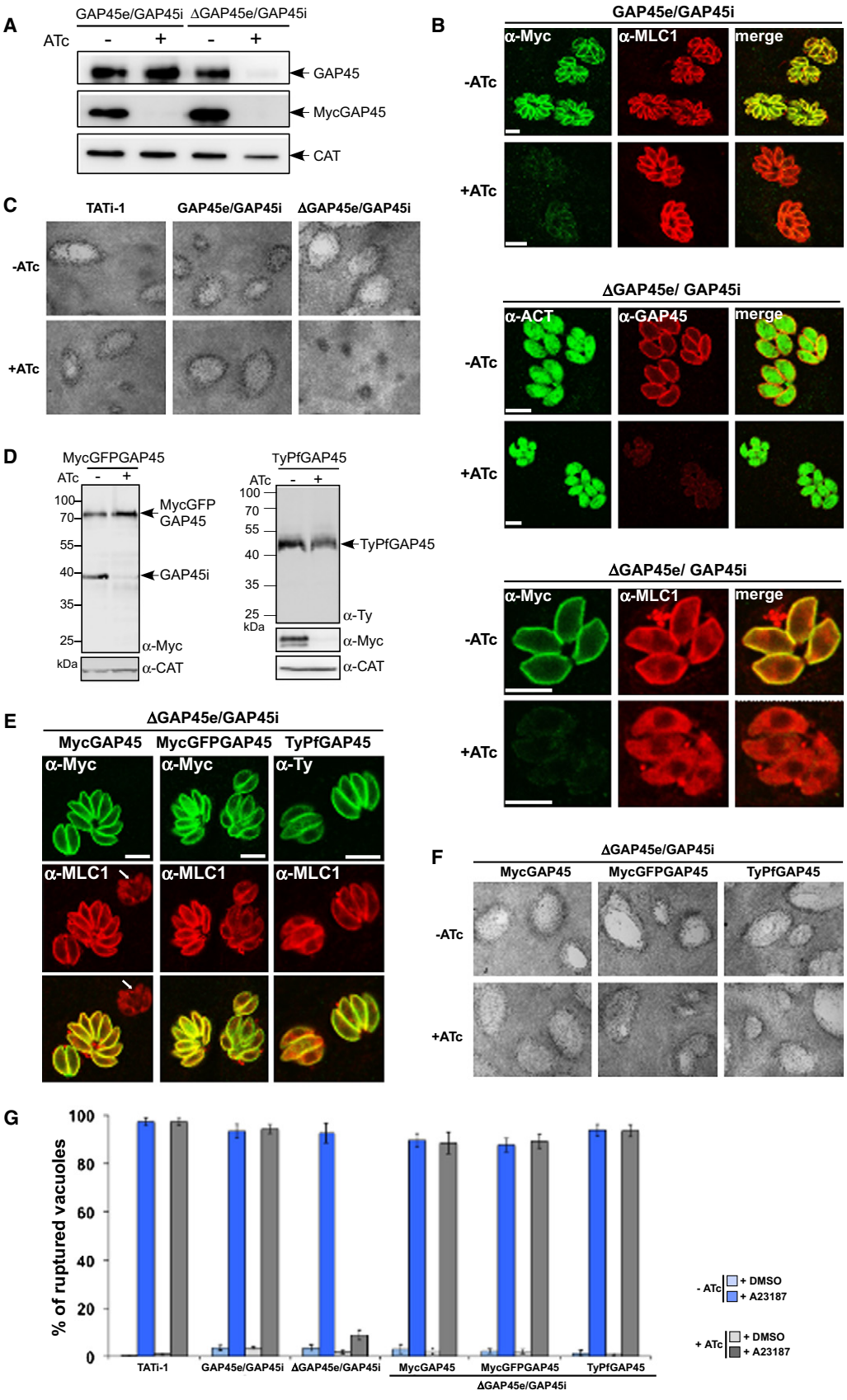
A
GAP45e/GAP45i
ΔGAP45e/GAP45i
ATc
GAP45
MycGAP45
CAT
B
GAP45e/GAP45i
α-Myc
α-MLC1
merge
-ATc
+ATc
ΔGAP45e/ GAP45i
α-ACT
α-GAP45
C
TATi-1
GAP45e/GAP45i
ΔGAP45e/GAP45i
D
MycGFPGAP45
TyPfGAP45
MycGFP GAP45
GAP45i
α-Myc
α-CAT
α-Ty
kDa
E
ΔGAP45e/GAP45i
MycGAP45
MycGFPGAP45
TyPfGAP45
α-MLC1
F
G
% of ruptured vacuoles
+ DMSO
+ A23187

phenotype excluded any impact of these coiled-coil mutants on parasite division (Figure S5C). The fact that TyGAP45Δcoil recruits the motor but failed to complement GAP45i depletion provides an additional hint for a second role of GAP45.

Mutations of the two conserved C-terminal cysteine residues (TyGAP45CC-AA) were shown in RH (Figure 4D) to prevent GAP45 association with the IMC; nevertheless, this mutant was still able to anchor to the PM and position the motor properly at the pellicle (Figure 6B). Rather unexpectedly, this mutant functionally complemented GAP45i depletion by plaque and egress assays (Figures 6C and 6D). These results suggest that interaction of GAP45 with the IMC is not absolutely required for glideosome function. To confirm this view, we performed an IP of the glideosome from metabolically labeled parasites. While MLC1 and MyoA were still part of the complex assembled with TyGAP45CC-AA, GAP50 and GAP40 were absent (Figure 6E). In contrast, TyGAP45Δcoil and TyPfGAP45 assembled as an intact MyoA-MLC1-GAP50-GAP40 complex. TyPfGAP45 exhibited the same pattern of multiple bands as in *P. falciparum*, suggesting that similar posttranslational modifications occur in *T. gondii.* The absence of motor assembly observed with TyGAP45-2coils by IFA was confirmed by coIP (Figure 6E). TyGAP45CC-AA assembled poorly with MyoA in absence of ATc probably due to its weaker affinity for MLC1 compared to the inducible copy of GAP45. In contrast, in the presence of ATc, TyGAP45CC-AA associated efficiently with MLC1-MyoA but still failed to interact with GAP50 and GAP40 (Figure 6F). Nevertheless MLC1 segregated with the IMC upon aerolysin treatment, suggesting that the motor is firmly anchored to the IMC, thereby explaining why the glideosome functions were rescued (Figure 6G).

GAP45 Plays a Key Role in Maintaining the Cohesion of the Pellicle during Invasion

The importance of N-terminal acylations and the length of the coiled-coil domain in GAP45 function were suggestive of a key second role besides recruitment of the motor to the IMC. We hypothesized that the interaction of GAP45 with both IMC and PM could have a structural significance especially in maintaining a fixed distance and tight connection between the two membranes in the context of the tensions imposed during gliding motility and invasion. A detailed EM analysis of parasites depleted in GAP45 or expressing mutants that failed to complement the phenotype revealed two major morphological alterations at the level of the pellicle. First, a deformation and irregular spacing between IMC and PM was observed in parasites lacking GAP45 or expressing the defective mutants in GC-AAMyc-GAP45 and coiled-coil mutants (Figures S6E–S6G). In contrast, MycGAP45 or TyGAP45CC-AA exhibited wild-type regular pellicle morphology (Figures S6A–S6C). A second striking phenotype is the accumulation of extra IMC membranes at the posterior pole of the postinvasion parasites (Figures S6H and S6I). This appears to be a consequence of the tension generated on the pellicle during invasion when the host-receptor/parasite-ligand complexes at the PM are translocated to the rear of the parasite, and the parasite is propelled forward into the host cell by the actomyosin system anchored to the IMC. In some extreme cases, the PM is considerably detached form the IMC (Figure S6J). The absence of GAP45 is detrimental to the maintenance of a link between the PM and the IMC.

GAP70 Is a Functional Homolog of GAP45 Tailored for the Apical Cap

A search in the *T. gondii* genome database revealed the presence of a gene closely related to *GAP45* that exhibits the same modular composition including the conserved N-terminal region with predicted acylation sites, a coiled-coil domain (longer than in GAP45) and a conserved C terminus (Figure S7A). In contrast to *GAP45*, which is ubiquitously found in all Apicomplexans, this gene is exclusively present in coccidians. Despite a predicted molecular mass of 37.6 kDa, the epitope-tagged protein migrated at 70 kDa on SDS-PAGE and hence was named GAP70 (Figure 7A). The same abnormal migration behavior was previously reported for GAP45 (Gaskins et al., 2004) and is possibly explained by the high content in negatively charged residues.

A series of tagged and truncated constructs established that, like GAP45, GAP70 is dually anchored to the PM via N-terminal acylations (Figures S7B and S7C) and to the apical cap via its C-terminal block (Figure 7B). Furthermore, GAP70 was also excluded from the nascent apical cap of the daughter cells unless an N-terminal tag interfering with myristoylation and palmitoylation was inserted (MycGAP70) (Figure 7B). This result is analogous to GAP45 and further consolidates our view that acylations prevent the anchoring of these proteins to the immature IMC. Finally, the C-terminal conserved region of GAP70 (aa 263 to 313) was sufficient to target GFP to the IMC although in this latter case to the restricted apical cap of IMC (MycHisGFPCtGAP70) (Figure 7B). Intriguingly, overexpression of GAP70 significantly affected the distribution of endogenous

Figure 5. Generation, Phenotypic Characterization and Functional Complementation of GAP45-iKO

(A) Western blot analysis of GAP45e/GAP45i and ΔGAP45e/GAP45i after 48 hr ± ATc. The downregulation of GAP45i was determined with anti-Myc antibody, and the deletion of GAP45e locus was confirmed by probing with anti-GAP45. Detection of catalase (CAT) was used as a loading control.

(B) IFA analysis of GAP45e/GAP45i and ΔGAP45e/GAP45i after 48 hr ± ATc. The upper panel shows the downregulation of GAP45i in presence of ATc, the middle panel shows the disappearance of GAP45e in the conditional KO, and the bottom panel shows the localization of MLC1 in ΔGAP45e/GAP45i. Scale bars represent 5 μm.

(C) Plaque assays were performed by incubation of host cells with parasites for 6 days ± ATc.

(D) Expression of the GAP45 complementing constructs analyzed by western blot with anti-Myc and anti-Ty antibodies after incubation for 48 hr ± ATc.

(E) The localization of GAP45-complementing constructs and MLC1 was analyzed by IFA with anti-Myc or anti-Ty (green) and anti-MLC1 (red) 48 hr after ATc treatment. The white arrow points to a noncomplemented ΔGAP45e/GAP45i vacuole. Scale bars represent 5 μm.

(F) Plaque assays were performed by incubation of complemented strains for 6 days ± ATc.

(G) Ionophore-induced egress assays were carried out with parasites cultured for 56 hr ± ATc before treatment with DMSO or Ca^{2+}-ionophore A23187 for 5 min. The results are expressed as a percentage of ruptured vacuoles and graphed as mean ± SEM.

See also Figure S4.

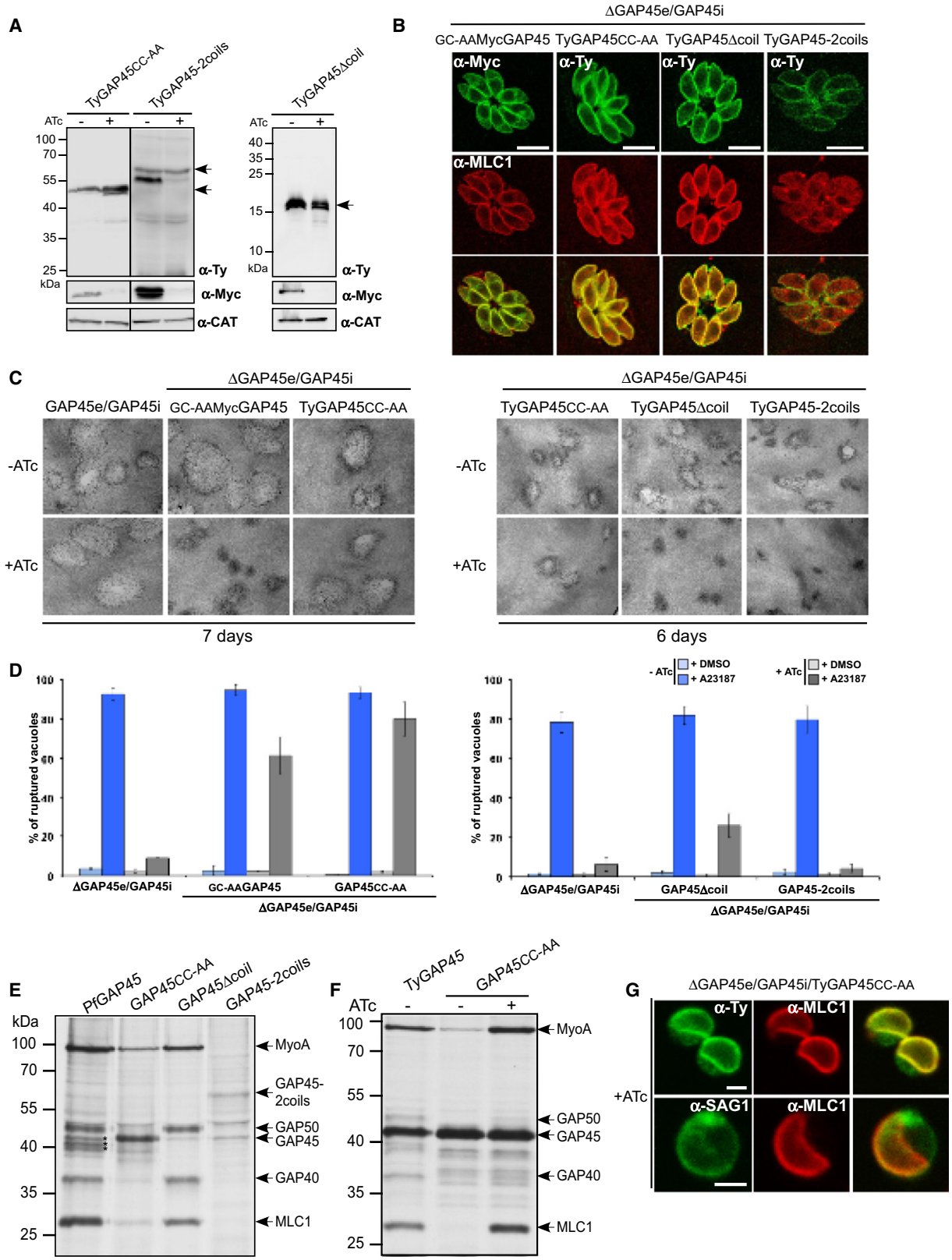

Figure 6. A Dual Role of GAP45 in Glideosome Function

(A) Expression of GAP45 complementing constructs was analyzed by western blot with anti-Myc and anti-Ty antibodies, after culture for 48 hr ± ATc.

(B) Localization of GAP45 complementing constructs and MLC1 were determined by IFA with anti-Myc or anti-Ty and anti-MLC1 antibodies after 48 hr in presence of ATc. Scale bars represent 5 μm.

GAP45 as shown by its local exclusion from the apical and posterior poles of the parasite (Figure 7B).

Given the striking similarities between these two proteins, we reasoned that the longer coiled-coil of GAP70 could be considered as a natural mutant for GAP45 and its substitution would generate a milder and more informative phenotype that the coiled-coil mutants.

To examine the potential of GAP70 to complement ΔGAP45e/GAP45i, we generated two constructs and introduced them into the ΔGAP45e/GAP45i using phleomycin selection. The full-length GAP70, with an internal Ty tag (TyGAP70), was compared to a chimera consisting of GAP70 with its C-terminal region replaced by the corresponding region from GAP45 (TyGAP70Ct45). By IFA, TyGAP70 was concentrated at the apical cap but also distributed throughout the entire pellicle, whereas TyGAP70Ct45 showed the typical homogenous distribution of GAP45. Plaque assays revealed that GAP70 has the capacity to partially substitute for GAP45 (Figure 7D). In both strains, recruitment of MLC1 to the pellicle was restored but in the case of TyGAP70, MLC1 was additionally concentrated to the apical cap (Figure S7D). These results validated the attribution of the name gliding-associated protein to this gene and showed that GAP70 is associated with to MLC1-MyoA. The presence of MyoA in TyGAP70 containing complex was shown by coIP with anti-Ty, using TyGAP45 as a control (Figure 7E). In contrast to *GAP45,* the *GAP70* gene could be disrupted conventionally by double crossing over (Figure S7E). The *gap70ko* showed no detectable phenotype by plaques assay, indicating that GAP70 is dispensable, possibly replaced by GAP45 (Figure S7H). In contrast, the amount of GAP70 is likely too limited to rescue the *gap45iko*. The morphology of the pellicle was examined by EM when GAP45 was substituted with GAP70. Interestingly, the spacing between IMC and PM was significantly increased as from 25.1 nm ± 1 in *gap45iko* complemented with MycGAP45 to 33.1 nm ± 4.1 in *gap45iko* complemented with TyGAP70 as measured on multiple EM samples and sections. This effect is consistent with the longer coiled-coil domain of GAP70 compared to GAP45 (Figure 7F).

DISCUSSION

In the first part of this study, we have identified a component of the glideosome, thereby defining that this machine is composed of five basic proteins (MyoA-MLC1-GAP45-GAP50-GAP40). The exact topology of this polytopic protein of the IMC and its contribution to the glideosome's function will await further experimental investigation.

MyoA lacks a tail but possesses a neck, which binds to MLC1. As recently reported (Heaslip et al., 2010), the N-terminal extension of MLC1 replaces the tail that usually binds to the cargo and brings MyoA to its site of action. We have mapped critical residues in the N-terminal extension of MLC1 that are important for its interaction with GAP45 and anchoring to the IMC. We demonstrated that the C-terminal domain of GAP45 is necessary and sufficient to recruit MLC1 and indirectly MyoA to the IMC. When fused to GFP, CtGAP45 leads to the anchoring of the motor to the IMC of the nascent daughter cells, probably via interaction with GAP50 and or GAP40. A premature anchoring of the motor is naturally prevented by the N-terminal lipid modifications of GAP45 that anchor the protein to the PM. Myristolylation is a modification that occurs very rapidly, even cotranslationally in the cytosol. It increases the affinity of the protein for membranes and hence can readily convert GAP45 into a substrate for a selective palmitoyl acyltransferase at the PM. Myristoyation and palmitoylation of GAP45 have been well documented in *P. falciparum* (Rees-Channer et al., 2006). Aerolysin treatment induces swelling of the parasites, imposing experimentally, a physical separation of the PM from the IMC. Since intact GAP45 is more firmly anchored to the IMC than to the PM, it was assumed to be located exclusively to the IMC. However, the different constructs examined here clearly established that GAP45 is anchored in the two components of the pellicle. As a word of caution, it is important to note that is it not known whether both interactions are occurring simultaneously. The space between the two membranes is only 20 to 25 nm, and although a modeling prediction of the coiled-coil domain of GAP45 suggests that it could span such a distance (data not shown), it would impose a considerable strain on the protein.

In the second part of this study, we undertook a functional dissection of GAP45 in order to assess the unique molecular features of this protein and their contribution to glideosome function. GAP45 is vital for gliding, invasion, and egress but does not contribute to parasite replication, although MyoA was recently implicated in parasite replication (Agop-Nersesian et al., 2009). The conditional knockout of GAP45 was exploited to determine the importance of acylations as well as the length and rigidity of GAP45 for its function. The results recapitulated in Table S1 are highlighting a dual role for GAP45. Despite the fact that GC-AA-MycGAP45 appropriately recruits the motor to the IMC, the glideosome functions are significantly impaired. In consequence, the anchor of GAP45 to the PM plays a crucial role in the cohesion of the pellicle. It is plausible that the translocation of the MICs-host receptor complexes to the posterior pole of the parasites imposes a considerable tension on the two membranes of the pellicle. The PM must move along with the

(C) Plaque assays performed by incubating host cells with complemented strains of ΔGAP45e/GAP45i for 6 or 7 days ± ATc.
(D) Ionophore-induced egress assay of complemented ΔGAP45e/GAP45i strains cultured for 56 hr ± ATc before treatment with DMSO or Ca^{2+}-ionophore A23187 for 5 min. The results are expressed as a percentage of ruptured vacuoles and graphed as mean ± SEM.
(E) [^{35}S]-labeled methionine/cysteine GAP45-iKO parasites stably expressing TyPfGAP45, TyGAP45CC-AA, TyGAP45Δcoil, and TyGAP45-2coils were cultured without ATc and subjected to IPs with anti-Ty antibodies. Eluted proteins were visualized by autoradiography. TyPfGAP45 is indicated by asterisks.
(F) Parasites expressing TyTgGAP45 were cultured in [^{35}S]-labeled methionine/cysteine medium without ATc and GAP45-iKO parasites complemented with TyGAP45CC-AA were cultured in the same medium ± ATc for 48 hr. The lysates were IP with anti-Ty antibodies and the elutions were visualized by autoradiography.
(G) GAP45-iKO parasites stably expressing TyGAP45CC-AA were cultured for 48 hr in presence of ATc. Freshly egressed, they were treated extracellularly with aerolysin and analyzed by IFA with anti-Ty, anti-MLC1, and anti-SAG1 antibodies. Scale bars represent 2 μm.
See also Figure S5 and S6.

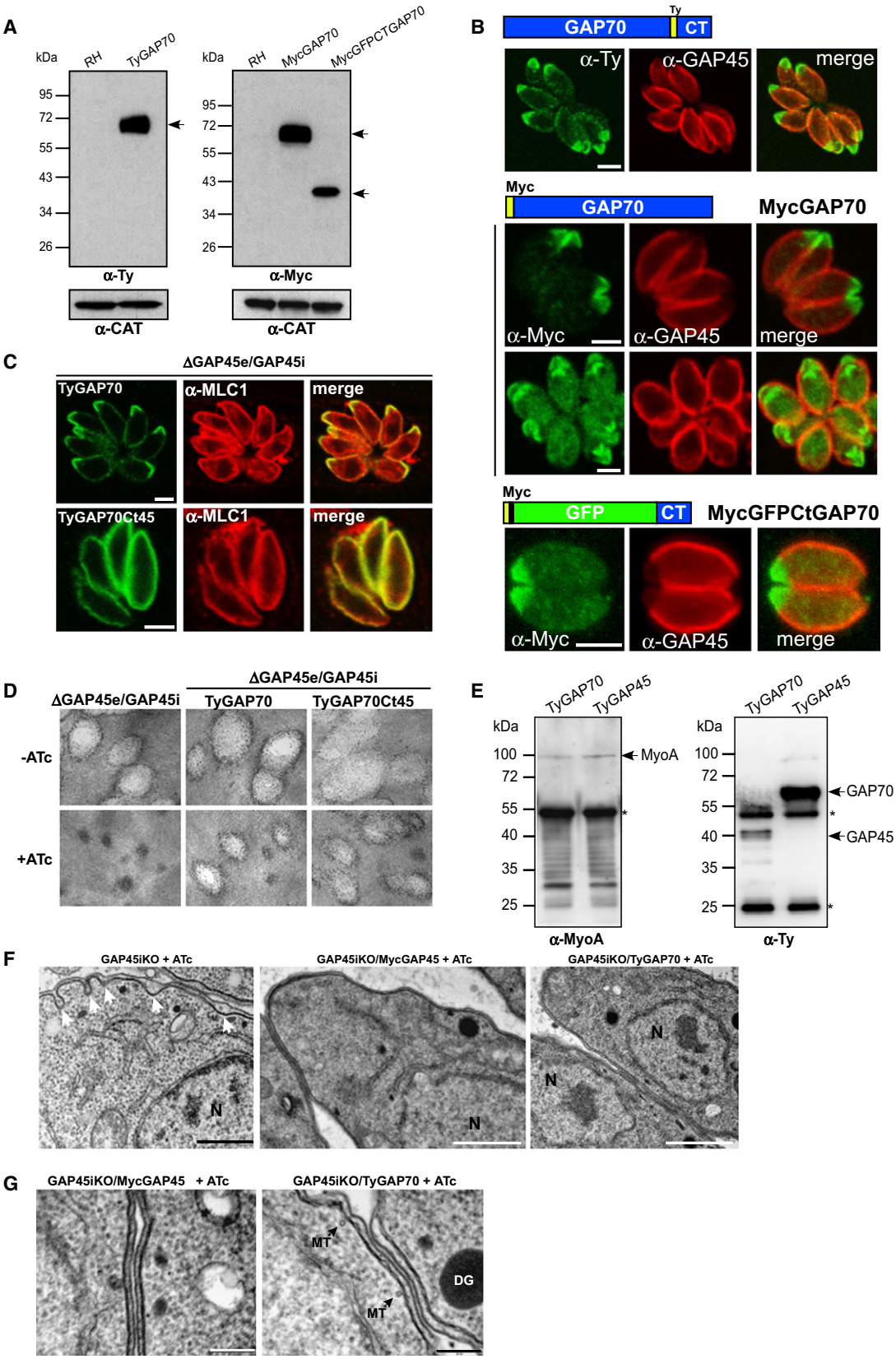
A
kDa
RH
TyGAP70
95
72
55
43
34
26
α-Ty
α-CAT
kDa
RH
MycGAP70
MycGFPCTGAP70
95
72
55
43
34
26
α-Myc
α-CAT
B
Ty
GAP70
CT
α-Ty
α-GAP45
merge
Myc
GAP70
MycGAP70
α-Myc
α-GAP45
merge
Myc
GFP
CT
MycGFPCtGAP70
α-Myc
α-GAP45
merge
C
ΔGAP45e/GAP45i
TyGAP70
α-MLC1
merge
TyGAP70Ct45
α-MLC1
merge
D
ΔGAP45e/GAP45i
ΔGAP45e/GAP45i
TyGAP70
TyGAP70Ct45
-ATc
+ATc
E
TyGAP70
TyGAP45
kDa
100
72
55
40
35
25
MyoA
*
α-MyoA
TyGAP70
TyGAP45
kDa
100
72
55
40
35
25
GAP70
*
GAP45
*
α-Ty
F
GAP45iKO + ATc
N
GAP45iKO/MycGAP45 + ATc
N
GAP45iKO/TyGAP70 + ATc
N
N
G
GAP45iKO/MycGAP45 + ATc
GAP45iKO/TyGAP70 + ATc
MT
MT
DG

IMC with respect to the extracellular matrix or the moving junction during gliding or invasion, respectively. GAP45 might constitute a fluid bridge between the IMC and PM such that the cohesion of the pellicle is maintained. Additionally, GAP45 could act as a spring between the two membranes to keep them at a suitable distance allowing the motor to function optimally. To experimentally test this hypothesis, we generated mutants that imposed a change on the length and rigidity between the N and C terminus of GAP45 either by deleting the coiled-coil domain or by duplicating it. In the case of TyGAP45Δcoil, access to the pellicle was not compromised and the motor was recruited but failed to complement. In contrast, in the absence of GAP45i, TyGAP45-2coils was excluded from the pellicle. These results indicated that the rigidity and length of GAP45 matter. Interestingly, the coccidians possess a natural mutant of GAP45, since the GAP70 differs from GAP45 mainly by the length of its coiled-coil. This GAP shares several identical features with GAP45 and hence proved a useful reference to confirm the properties reported here for GAP45. Despite the considerable similarities between the two proteins, GAP70 distinguished itself by a tightly restricted localization to the apical cap, a subdomain of the IMC only found in parasites harboring a conoid. At this stage, it is tempting to speculate that the variable length of their coiled-coil domains reflects a refined adaptation to accommodate a change in the tension and or the distance between the IMC and PM that might be imposed by the curvature of the pellicle at the proximity of the apical pole.

The fact that *TgGAP70* is dispensable suggests that *TgGAP45* can functionally replace it or that the protein has a more pronounced contribution at a different stage. On the contrary, depletion of GAP45 exhibits one of the most profound phenotypes among the invasion related genes analyzed so far by the conditional knockout strategy. The amount of endogenously produced GAP70 is clearly insufficient to complement for the absence of GAP45. Furthermore, overexpression of TyGAP70 and TyGAP70Ct45 failed to rescue the phenotype back to wild-type level, indicating that the length of the coiled-coil domain is critical for the structural role of GAP45. Morphological examination of the substitution of GAP45 with GAP70 revealed a significant impact on the distance between IMC and PM consistent with the increased length of GAP70.

Taken together, these results reinforce the notion that these GAP45 and GAP70 play a role in pellicle cohesion during motility and invasion. MyoA is firmly anchored to the IMC, itself connected to the cytoskeleton composed of the subpellicular basket of microtubules. GAP50 was proposed to act as a firm anchor on the basis of recent FRET analysis experiments (Johnson et al., 2007), and with its nine transmembrane spanning domains, GAP40 could also accomplish this task. Other proteins such as the GAPMs might contribute to the overall rigidity and flattened shape of the IMC (Bullen et al., 2009). In a recent study, two serine residues (S163 and S167) positioned in the conserved C-terminal domain of GAP45 were shown to be phosphorylated and this posttranslational modification was reported to be important to control the final step in assembly of the myosin XIV motor complex with GAP50 (Gilk et al., 2009). Here, the mutant MycGAP45CC-AA efficiently recruits the motor to the IMC and is functional. However this mutant has lost its ability to bind to GAP50 and GAP40, suggesting that this interaction is dispensable.

The fact that *P. falciparum* GAP45 fully restores the glideosome function to wild-type level has several implications. It highlights once again the extent to which the gliding machinery is conserved across the phylum of *Apicomplexa*. *Plasmodium* GAP45 not only interacts with the *Toxoplasma* MLC1, GAP50, and GAP40, but also acts as an appropriate substrate for the enzymes involved in the posttranslational modifications such as the palmitoyltransferase(s), kinase(s), and phosphatase(s). This study sheds light on glideosome assembly and function uncovering two pivotal roles for GAP45: (1) the recruitment of the motor to the pellicle and its appropriate insertion into the IMC of mature parasite and (2) a structural function by maintaining together the IMC and PM during gliding motility and invasion.

EXPERIMENTAL PROCEDURES

Cloning of DNA Constructs

All amplifications were performed with La Taq (TaKaRa) and primers listed in Table S2. The description of the cloning strategies used in this study is detailed in the Supplemental Experimental Procedures.

T. gondii Culture

T. gondii tachyzoites were grown in confluent HFFs or in Vero cells maintained in Dulbecco's Modified Eagle's Medium (DMEM; GIBCO, Invitrogen) supplemented with 10% fetal calf serum, 2 mM glutamine, and 25 μg/ml gentamicin.

Parasite Transfection and Selection of Stable Transformants

Parasite transfections and selection of transgformants were performed as previously reported (Plattner et al., 2008) TATi-1 parasites (Meissner et al., 2002) have been cotransfected with 80 μg pTetO7Sag4MycGAP45 vector

Figure 7. GAP70, a Glideosome-Associated Protein

(A) Western blot analysis of the stable strains stably expressing TyGAP70, MycGAP70 and MycHisGFPCtGAP70. The CAT was used as a loading control. TgGAP70 (GenBank HM117968).

(B) The localization of TyGAP70, MycGAP70, and MycHisGFPGAP70 was analyzed by IFA in intracellular parasites with anti-Ty or anti-Myc. GAP45 stained the periphery of the parasites. Scale bars represent 2 μm.

(C) The localization of the complementing copy of TyGAP70 and TyGAP70Ct45 in the ΔGAP45e/GAP45i background was determined by IFA with anti-Ty antibody on intracellular parasites treated for 48 hr with ATc. The ability of these proteins to restore the peripheral localization of MLC1 was assessed with anti-MLC1 antibody.

(D) Plaque assays were performed by incubation of host cells with ΔGAP45e/GAP45i and complemented ΔGAP45e/GAP45i strains for 7 days ± ATc.

(E) CoIPs were performed on parasites stably expressing TyGAP70 and TyGAP45 with anti-Ty antibodies, and elutions were analyzed by western blot with anti-MyoA and anti-Ty in the left and right panels, respectively.

(F) Electron micrographs of ΔGAP45e/GAP45i parasites (left), complemented with MycGAP45 (middle) and with TyGAP70 (right) after 24 hr + ATc. Scale bars represent 0.5 μm (left and middle) and 1 μm (right).

(G) The pellicle of ΔGAP45e/GAP45i parasites complemented MycGAP45 (left) and GAP70Ty (right) and treated with ATc for 48 hr was analyzed by electron microscopy. Scale bars represent 0.2 μm.

See also Figure S7.

(linearized with NotI) and 20 μg pTub5CAT vector. Twenty micromolar chloramphenicol have been added to the culture medium to select the resistant parasites. The positive parasites were then tranfected with 60, 80, and 100 μg p2854-DHRF-5′3′TgGAP45 (linearized with SbfI). One microgram per mililiter pyrimethamine has been used to select the resistant parasites. ΔGAP45e/GAP45i strain was complemented with 80 μg pTUB8MycGAP45, pTUB8-MycGFPGAP45, and pTUB8TyPfGAP45 under anhydrotetracycline (ATc) selection. ΔGAP45e/GAP45i strain was complemented with 80 μg pTUB8GC-AAMycGAP45-HX, pTUB8TyGAP70-HX, or pTUB8Ty-GAP70Ct45-HX vectors, and 20 μg pT/230ble vector (Soldati et al., 1995) or with 80 μg pTUB8TyGAP45CC-AA-bleo, pTUB8TyGAP45-2coils-bleo, and pTUB8GAP45TyΔcoil-bleo under phleomycin selection performed by incubation of extracellular tachyzoites with 10 to 30 μg/ml phleomycin for 4 hr at 37°C.

Antibodies

The antibodies used in these study were described before as follows: polyclonal rabbit α-CAT (Ding et al., 2000), α-GAP45 (Plattner et al., 2008), α-MyoA (Hettmann et al., 2000), α-MLC1, and α-ACT (Herm-Götz et al., 2002). The Ty and c-Myc tags were detected with the monoclonal mouse α-Ty (BB2) and α-Myc (mAb 9E10), respectively.

Activation and Use of *Aeromonas hydrophila* Aerolysin

Prior to use, purified recombinant protoxin was activated for 15 min at 37°C in 100 μl PBS with 4 μl trypsin diluted at 1 mg/ml into HBS (140 mM NaCl, 2.7 mM KCl, 20 mM HEPES [pH 7.4]). For experiments, freshly harvested parasites were washed with PBS and incubated for 10 min at 37°C on coverslips coated with poly-L-lysine. Parasites were then treated with aerolysin at 80–100 ng/ml for 4 hr at 37°C before fixation.

Immunofluorescence Assay and Confocal Microscopy

Extracellular parasites treated or untreated with aerolysin and parasites-infected HFFs were fixed with 4% paraformaldehyde (PFA) or 4% PFA/0.05% glutaraldehyde (PFA/GA) in PBS, depending of the antigen to be labeled and processed as previously described (Hettmann et al., 2000). Confocal images were collected with a Leica laser scanning confocal microscope (TCS-NT DM/IRB and SP2) using a 1003 Plan-Apo objective with NA 1.4.

Plaque Assay

Host cells were infected with parasites ± 1 μg/ml ATc for 6 or 7 days before fixation with PFA/GA followed by Giemsa staining.

Egress Assay

Parasites were treated for 24 hr ± ATc before egress, inoculated on new HFFs, and allowed to grow for 33 hr ± ATc. Parasites-infected HFFs were then incubated for 5 min at 37°C with DMEM containing 0.06% DMSO or 3 μM Ca^{2+} ionophore A23187 from *Streptomyces chartreusensis* (calbiochem) before fixation. Double IFA were performed with α-GRA3 and α-SAG1 antibodies. The average number of ruptured vacuoles was determined by counting 100 vacuoles for each condition and for at least two independent experiments.

Metabolic Labeling and Coimmunoprecipitation of the Glideosome Complex

HFFs were heavily infected with freshly released parasites and washed several hours later. After 30 hr, cells were incubated in methionine/cysteine-free DMEM (sigma) for 1 hr before incubation in DMEM containing 50 μCi [^{35}S]-labeled methionine/cysteine (Hartmann analytic GmbH) per ml for 16 hr at 37°C. For coIPs, freshly released tachyzoites were harvested, washed in PBS, and lysed in coIP buffer (1% [v/v] Triton X-100, 50 mM Tris-HCl [pH 8], 150 mM NaCl) in presence of a protease inhibitor cocktail (Roche). Cells were frozen and thawed, sonicated on ice, incubated for 10 min on ice, and centrifuged at 14,000 rpm for1 hr at 4°C. Supernatants were then subjected to IP as already described (Gaskins et al., 2004).

Subcellular Fractionations

Freshly released tachyzoites were harvested, washed in PBS, and then resuspended into PBS, PBS and 1% Triton X-100, PBS and 1M NaCl, or PBS and 0.1 M Na_2CO_3 [pH 11.5]. Parasites were lysed by freezing and thawing followed by sonication on ice. Pellet and soluble fractions were separated by centrifugation for 1 hr at 14,000 rpm at 4°C. The solubility of CAT was checked in the different conditions as control.

Transmission Electron Microscopy and Measure of Distances

Parasites were treated for 24 hr ± ATc prior egress, transferred on new HFFs, and allowed to grow 24 more hr ± ATc. Cells were trypsinized and resuspended in PBS. Parasite pellets were fixed with 2.5% glutaraldehyde in 0.1 M phosphate buffer, postfixed in osmium tetroxide, dehydrated in ethanol, and treated with propylene oxide prior to embedding in epon resin. Thin sections were stained with uranyl acetate and lead citrate prior to examining in a Technai 20 electron microscope (FEI Company). Electron micrographs of GAP45iKO complemented with MycGAP45 and TyGAP70 (+ATc) taken with a magnification of 97,000 were analyzed in Photoshop CS4 (Adobe). Nine membrane pictures for each strain were used to determine the distance between the PM and the IMC by drawing an average of 20 lines/membrane.

ACCESSION NUMBERS

The Genbank accession numbers for the GAP40 and GAP70 sequences reported in this paper are HM751080 and HM117968, respectively.

SUPPLEMENTAL INFORMATION

Supplemental Information includes Supplemental Experimental Procedures, seven figures, and two tables and can be found with this article online at doi:10.1016/j.chom.2010.09.002.

ACKNOWLEDGMENTS

We thank J. Curran and T. Soldati for critical reading of the manuscript, D. Jacot constructive discussions, and G. Rugarabamu for assistance. We thank L. Abrami and G. Van der Goot for providing purified aerolysin and G. Ward for the anti-IMC1 antibodies. The research leading to these results has received funding from the Swiss National Foundation (FN3100A0-116722) and the European Community's Seventh Framework Programme (FP7/2007-2013) under grant agreement number 242095. D.S. is an international scholar of the Howard Hughes Medical Institute.

Received: April 7, 2010
Revised: July 26, 2010
Accepted: September 3, 2010
Published: October 20, 2010

REFERENCES

Agop-Nersesian, C., Naissant, B., Ben Rached, F., Rauch, M., Kretzschmar, A., Thiberge, S., Menard, R., Ferguson, D.J., Meissner, M., and Langsley, G. (2009). Rab11A-controlled assembly of the inner membrane complex is required for completion of apicomplexan cytokinesis. PLoS Pathog. *5*, e1000270.

Bergman, L.W., Kaiser, K., Fujioka, H., Coppens, I., Daly, T.M., Fox, S., Matuschewski, K., Nussenzweig, V., and Kappe, S.H. (2003). Myosin A tail domain interacting protein (MTIP) localizes to the inner membrane complex of Plasmodium sporozoites. J. Cell Sci. *116*, 39–49.

Black, M., Seeber, F., Soldati, D., Kim, K., and Boothroyd, J.C. (1995). Restriction enzyme-mediated integration elevates transformation frequency and enables co-transfection of *Toxoplasma gondii*. Mol. Biochem. Parasitol. *74*, 55–63.

Bosch, J., Turley, S., Roach, C.M., Daly, T.M., Bergman, L.W., and Hol, W.G. (2007). The closed MTIP-myosin A-tail complex from the malaria parasite invasion machinery. J. Mol. Biol. *372*, 77–88.

Bullen, H.E., Tonkin, C.J., O'Donnell, R.A., Tham, W.H., Papenfuss, A.T., Gould, S., Cowman, A.F., Crabb, B.S., and Gilson, P.R. (2009). A novel family of Apicomplexan glideosome-associated proteins with an inner membrane-anchoring role. J. Biol. Chem. *284*, 25353–25363.

Ding, M., Clayton, C., and Soldati, D. (2000). *Toxoplasma gondii* catalase: are there peroxisomes in toxoplasma? J. Cell Sci. *113*, 2409–2419.

Dubremetz, J.F., and Torpier, G. (1978). Freeze fracture study of the pellicle of an eimerian sporozoite (Protozoa, Coccidia). J. Ultrastruct. Res. *62*, 94–109.

Gaskins, E., Gilk, S., DeVore, N., Mann, T., Ward, G., and Beckers, C. (2004). Identification of the membrane receptor of a class XIV myosin in *Toxoplasma gondii*. J. Cell Biol. *165*, 383–393.

Gilk, S.D., Gaskins, E., Ward, G.E., and Beckers, C.J. (2009). GAP45 phosphorylation controls assembly of the Toxoplasma myosin XIV complex. Eukaryot. Cell *8*, 190–196.

Green, J.L., Martin, S.R., Fielden, J., Ksagoni, A., Grainger, M., Yim Lim, B.Y., Molloy, J.E., and Holder, A.A. (2006). The MTIP-myosin A complex in blood stage malaria parasites. J. Mol. Biol. *355*, 933–941.

Heaslip, A.T., Leung, J.M., Carey, K.L., Catti, F., Warshaw, D.M., Westwood, N.J., Ballif, B.A., and Ward, G.E. (2010). A small-molecule inhibitor of *T. gondii* motility induces the posttranslational modification of myosin light chain-1 and inhibits myosin motor activity. PLoS Pathog. *6*, e1000720.

Herm-Götz, A., Weiss, S., Stratmann, R., Fujita-Becker, S., Ruff, C., Meyhöfer, E., Soldati, T., Manstein, D.J., Geeves, M.A., and Soldati, D. (2002). *Toxoplasma gondii* myosin A and its light chain: a fast, single-headed, plus-end-directed motor. EMBO J. *21*, 2149–2158.

Hettmann, C., Herm, A., Geiter, A., Frank, B., Schwarz, E., Soldati, T., and Soldati, D. (2000). A dibasic motif in the tail of a class XIV apicomplexan myosin is an essential determinant of plasma membrane localization. Mol. Biol. Cell *11*, 1385–1400.

Johnson, T.M., Rajfur, Z., Jacobson, K., and Beckers, C.J. (2007). Immobilization of the type XIV myosin complex in *Toxoplasma gondii*. Mol. Biol. Cell *18*, 3039–3046.

Keeley, A., and Soldati, D. (2004). The glideosome: a molecular machine powering motility and host-cell invasion by Apicomplexa. Trends Cell Biol. *14*, 528–532.

Meissner, M., Schlüter, D., and Soldati, D. (2002). Role of *Toxoplasma gondii* myosin A in powering parasite gliding and host cell invasion. Science *298*, 837–840.

Morrissette, N.S., Murray, J.M., and Roos, D.S. (1997). Subpellicular microtubules associate with an intramembranous particle lattice in the protozoan parasite *Toxoplasma gondii*. J. Cell Sci. *110*, 35–42.

Opitz, C., and Soldati, D. (2002). 'The glideosome': a dynamic complex powering gliding motion and host cell invasion by *Toxoplasma gondii*. Mol. Microbiol. *45*, 597–604.

Plattner, F., Yarovinsky, F., Romero, S., Didry, D., Carlier, M.F., Sher, A., and Soldati-Favre, D. (2008). Toxoplasma profilin is essential for host cell invasion and TLR11-dependent induction of an interleukin-12 response. Cell Host Microbe *3*, 77–87.

Rees-Channer, R.R., Martin, S.R., Green, J.L., Bowyer, P.W., Grainger, M., Molloy, J.E., and Holder, A.A. (2006). Dual acylation of the 45 kDa gliding-associated protein (GAP45) in *Plasmodium falciparum* merozoites. Mol. Biochem. Parasitol. *149*, 113–116.

Ren, J., Wen, L., Gao, X., Jin, C., Xue, Y., and Yao, X. (2008). CSS-Palm 2.0: an updated software for palmitoylation sites prediction. Protein Eng. Des. Sel. *21*, 639–644.

Soldati, D., Kim, K., Kampmeier, J., Dubremetz, J.F., and Boothroyd, J.C. (1995). Complementation of a *Toxoplasma gondii* ROP1 knock-out mutant using phleomycin selection. Mol. Biochem. Parasitol. *74*, 87–97.

Wetzel, D.M., Håkansson, S., Hu, K., Roos, D., and Sibley, L.D. (2003). Actin filament polymerization regulates gliding motility by apicomplexan parasites. Mol. Biol. Cell *14*, 396–406.

Wichroski, M.J., Melton, J.A., Donahue, C.G., Tweten, R.K., and Ward, G.E. (2002). *Clostridium septicum* alpha-toxin is active against the parasitic protozoan *Toxoplasma gondii* and targets members of the SAG family of glycosylphosphatidylinositol-anchored surface proteins. Infect. Immun. *70*, 4353–4361.